IOP Publishing Journal of Physics: Condensed Matter
J. Phys.: Condens. Matter **32** (2020) 225706 (7pp) https://doi.org/10.1088/1361-648X/ab73a4

Synthesis, structure and physical properties of new intermetallic spin glass-like compounds RE_2PdGe_3 (RE = Tb and Dy)

L S Litzbarski, T Klimczuk and M J Winiarski

Faculty of Applied Physics and Mathematics and Center for Future Materials, Gdansk University of Technology, Narutowicza 11/12, 80-233 Gdansk, Poland

E-mail: leszek.litzbarski@pg.edu.pl

Received 5 November 2019, revised 21 January 2020
Accepted for publication 6 February 2020
Published 5 March 2020

Abstract

New intermetallic compounds $Tb_2Pd_{1.25}Ge_{2.75}$ and $Dy_2Pd_{1.25}Ge_{2.75}$ have been synthesized using the arc-melting method. The crystallographic structure and magnetic, electronic transport, and thermal properties are reported. The crystal structure obtained from powder x-ray diffraction analysis suggests that these compounds crystallize in the AlB_2-type structure (space group P6/*mmm*, no. 191) with lattice parameters $a = 4.228\,53(5)/4.230\,54\ (2)$ Å and $c = 3.942\,25(9)/3.945\,52(5)$ Å for the compounds with Tb and Dy respectively. The ac and dc magnetic susceptibility studies reveal spin-glass like behavior, with freezing temperature $T_f = 10.5$ K for $Tb_2Pd_{1.25}Ge_{2.75}$ and 4.5 K for $Dy_2Pd_{1.25}Ge_{2.75}$. These data are in good agreement with the heat capacity measurements.

Keywords: spin glass, AlB_2-type compounds, intermetallic compounds

(Some figures may appear in colour only in the online journal)

Introduction

During the last few years, several compounds of the type RE_2TGe_3, where RE is a rare earth element and T is a transition metal, have been studied. These compounds have a crystal structure derived from that of AlB_2 and show interesting physical properties. For example Y_2PdGe_3 [1] is a superconductor with $T_c = 3$ K and Gd_2PdGe_3 exhibits antiferromagnetic order below 10 K [2].

Most of the reported intermetallic compounds in the RE_2PdGe_3 family crystalize in the hexagonal (*P6/mmm*) structure [1–4]. The hexagonal AlB_2 type structure represents one of the simplest inorganic structure types, with the unit cell consisting of only three atoms. The AlB_2 structure is composed of alternating hexagonal layers of Al and graphite-like honeycomb layers of B, as shown in figures 1(a) and (b) (all crystal structure drawings were produced using the VESTA program [5]). These boron layers are well separated from each other ($d_{inter} = c \approx 3.3$ Å) and the distance between contiguous boron atoms is defined by the lattice parameter a: $d_{intra} = a/\sqrt{3} \approx 1.7$ Å. It is possible to get AlB_2-related structures by substitution of aluminum atoms with a rare earth or actinoid metal and replacing boron by silicon or germanium, which generates a large family of binary compounds. In ternary compounds the hexagonal layer is made up of a transition metal and a main group element. Such compounds exist in two types of *P6/mmm* structure: the ordered variant, presented in figure 1(c), characterized by a lattice parameter ratio $c/a \approx 0.5$ (e.g. Ca_2PdGe_3) [6], and the disordered variant, which is shown in figure 1(d), with c/a about 1.

We have searched for new materials with long range magnetic ordering in the $RE(Pd, Ge)_2$ family and succeeded in the synthesis of spin-glass like $Tb_2Pd_{1.25}Ge_{2.75}$ and $Dy_2Pd_{1.25}Ge_{2.75}$. In this paper, we describe the synthesis, crystal structure and physical properties of these compounds.

Experimental

The synthesis of $RE_2Pd_{1+x}Ge_{3-x}$ ($x = 0$–0.35) was performed using an arc-melting method. Stoichiometric amounts of palladium (99.95%, Alfa Aesar) and germanium (99.999%, Alfa Aesar) were weighted. Due to the volatility of terbium (99.9%,

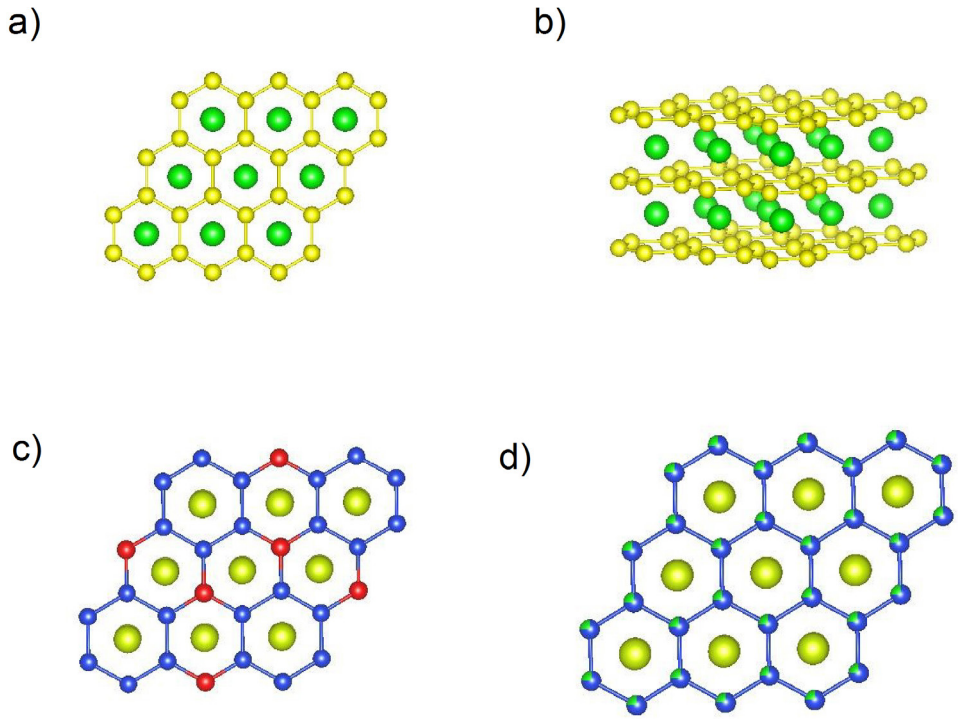

Figure 1. Crystal structure of three related compounds: (a) and (b) AlB_2—small and large balls are boron and aluminum; (c) Ca_2PdGe_3—large balls represent calcium, small red and blue balls are palladium and germanium; (d) Tb_2PdGe_3 large balls are terbium, small represents palladium and germanium, which occupy hexagonal site with probability 1:3.

Onyxmet) and dysprosium (99.9%, Onyxmet), these chemical elements were used in 2% molar excess. The mixture of Tb or Dy, Pd and Ge was melted together under a high purity, Zr-gettered, argon atmosphere in an arc furnace (MAM-1 GmbH Edmund Bühler). The polycrystalline ingot was turned several times to ensure homogenity. The total weight losses during the melting process were less than 0.5%.

The samples were characterized by powder x-ray diffraction obtained employing a Bruker D2Phaser diffractometer with CuK_α radiation, equipped with a XE-T detector. The results were processed by means of LeBail refinement using the FullProf software [7]. $Tb_2Pd_{1.25}Ge_{2.75}$ was also examined by EDS spectroscopy using a scanning electron microscope FEI Quanta FEG 250 to confirm the chemical composition of the obtained samples. Spectral data was processed using the EDAX TEAM software by means of the standardless eZAF analysis. The obtained results agreed with assumed stoichiometry within the accuracy of the employed method of analysis.

Samples of $Tb_2Pd_{1.25}Ge_{2.75}$ and $Dy_2Pd_{1.25}Ge_{2.75}$ were investigated by heat capacity, electrical transport and magnetic measurements using a Quantum Design physical property measurement system. The electrical resistivity measurements were performed using a standard four probe technique with an applied current of 5 mA. Electrical contacts were made by spot-welding platinum wires ($\phi = 50$ μm) on the sample surface. Magnetization was measured with various magnetic fields after field cooling (FC) and zero field cooling (ZFC). In the case of ac measurement of magnetic susceptibility, the ac measurement system was used. Susceptibility was approximated as sample magnetization divided by the applied magnetic field: $\chi \approx M/H$. Time evolution of magnetization was measured in ZFC mode, in which the sample is initially cooled down to relevant temperature and next a small amount of magnetic field is applied to start recording $M(t)$ data. The heat capacity data were obtained by using the thermal relaxation technique in the temperature range $1.9\,\mathrm{K} < T < 300\,\mathrm{K}$.

Results and discussion

Synthetized samples of $RE_2Pd_{1+x}Ge_{3-x}$ were investigated by powder x-ray diffraction (XRD). It was observed that for $x = 0.25$ samples were single-phase, while in other cases they were contaminated by a parasitic phase of 1:2:2 stoichiometry ($ThCr_2Si_2$ type structure). The sample of $Tb_2Pd_{1.25}Ge_{2.75}$ was studied by EDS spectroscopy and the average composition of the pellet is within an error of the nominal composition. XRD patterns (figure 2) confirmed that $Tb_2Pd_{1.25}Ge_{2.75}$ crystallizes in the AlB_2-type hexagonal structure. Unlike Ca_2PdGe_3 [6], $Tb_2Pd_{1.25}Ge_{2.75}$ shows no superstructure reflections, suggesting a statistical disorder within the Pd–Ge plane. The same observation had been made for $Dy_2Pd_{1.25}Ge_{2.75}$. Structural parameters, which were calculated by Le Bail refinements, are gathered in table 1. Received values are close to those for Gd_2PdGe_3 [2], Nd_2PdGe_3 and Y_2PdGe_3 [3]. It can be observed that the volume of a unit cell is growing with the increase of the atomic radius of the rare earth metal in RE_2PdGe_3 compounds.

An anisotropic broadening effect was observed in the XRD pattern, the $00l$ reflections being far more broadened than others. This may suggest a presence of stacking faults in the structure, the anisotropic strain distribution, or a combination

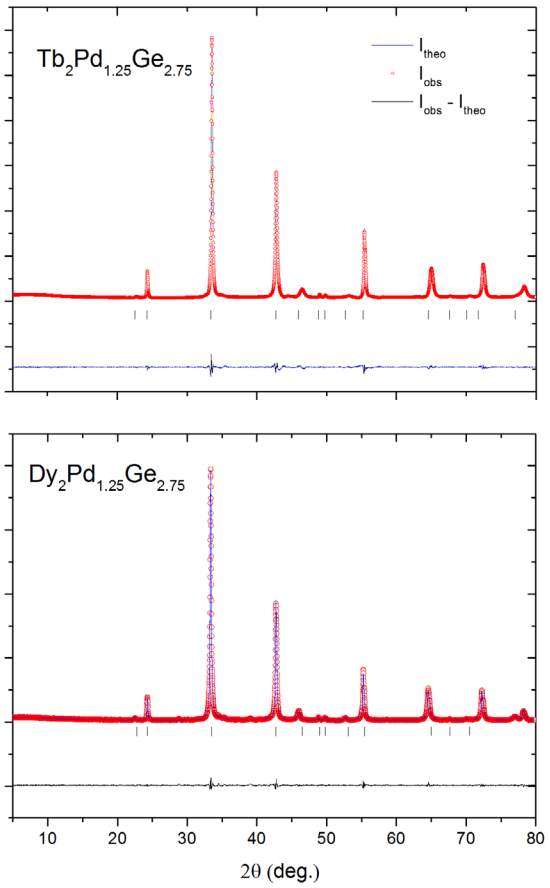

Figure 2. Le Bail refinement of powder XRD data for $Tb_2Pd_{1.25}Ge_{2.75}$ and $Dy_2Pd_{1.25}Ge_{2.75}$ Observed data and calculated intensity are represented by red circles and blue lines respectively. Black vertical ticks correspond to Bragg peaks for space group P6/*mmm* (no. 191).

Table 1. Refined structural parameters for $Tb_2Pd_{1.25}Ge_{2.75}$ and $Dy_2Pd_{1.25}Ge_{2.75}$.

Refined formula	$Tb_2Pd_{1.25}Ge_{2.75}$	$Dy_2Pd_{1.25}Ge_{2.75}$
Space group	*P6/mmm* (No.191)	
a (Å)	4.226 05(6)	4.230 48 (5)
c (Å)	3.904 58(11)	3.945 26(8)
V (Å^3)	60.391(2)	61.149(2)
Molar weight (g mol^{-1})	657.78	650.63
Density (g cm^3)	5.44	5.32
Tb (1a)	$x = y = z = 0$	
Pd (2d)	$x = 1/3$ $y = 2/3$ $z = 0.5$	
Ge (2d)	$x = 1/3$ $y = 2/3$ $z = 0.5$	
Figures of merit:		
R_p (%)	10.2	8.70
R_{wp} (%)	10.6	9.67
R_{expt} (%)	6.11	5.73
χ^2	3.01	2.91

of both. In order to improve the LeBail fit, the effect was modelled using the quartic model of anisotropic strain implemented in Fullprof [8].

Figure 3 shows the temperature dependence of magnetic susceptibility measured at $\mu_0 H = 0.1$ T for (a) $Tb_2Pd_{1.25}Ge_{2.75}$ and (b) $Dy_2Pd_{1.25}Ge_{2.75}$. $\chi(T)$ increases with decreasing

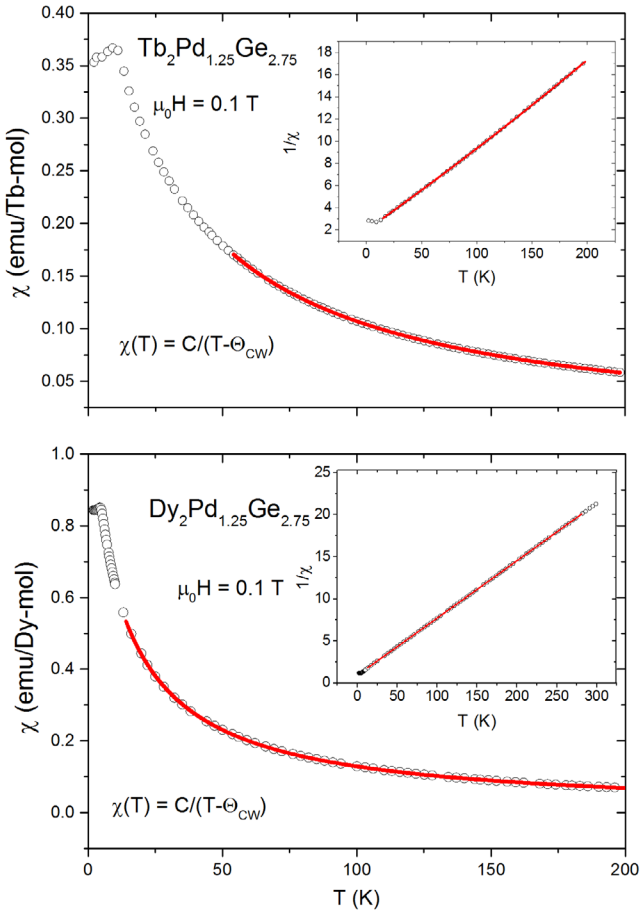

Figure 3. The temperature dependence of the magnetic susceptibility for $Tb_2Pd_{1.25}Ge_{2.75}$ and $Dy_2Pd_{1.25}Ge_{2.75}$. The red line is a fit to a Curie–Weiss law for temperatures above 50 K and 25 K respectively. The inset shows the inverse magnetic susceptibility as a function of temperature with the fitted function $1/\chi = T/C - \theta_{cw}/C$ (red line).

temperature, which is typical behavior for Curie–Weiss paramagnets. Plots of inverse magnetic susceptibility versus temperature are shown in insets. The plot for the sample containing dysprosium is linear in the range $T = 25$–300 K, and thus it is fitted with a dependence formulated with the Curie–Weiss law in this range. The plot of inverse of χ versus T for the compound with terbium is found to be linear above 50 K and it is also fitted with a Curie–Weiss law. Obtained values of the paramagnetic Curie temperature (θ_{cw}) and Curie constant (C) are gathered in table 2. The effective magnetic moment was calculated using equation:

$$\mu_{eff} = \left(\frac{3Ck_B}{\mu_B^2 N_A}\right)^{1/2},$$

where k_B is the Boltzmann constant, μ_B is the Bohr magneton and N_A is the Avogadro number. The resulting μ_{eff} is slightly larger than theoretical value for Tb^{3+} free ion (9.72 μ_B) [9], which may be caused by a small magnetic moment induced on Pd. In the case of $Dy_2Pd_{1.25}Ge_{2.75}$ the calculated value of the effective magnetic moment is close to the theoretical value for Dy^{3+} (10.65 μ_B) [9], which is consistent with the trivalent nature of the dysprosium ion. The low temperature FC and ZFC

Table 2. Selected physical property data for $Tb_2Pd_{1.25}Ge_{2.75}$ and $Dy_2Pd_{1.25}Ge_{2.75}$.

	$Tb_2Pd_{1.25}Ge_{2.75}$	$Dy_2Pd_{1.25}Ge_{2.75}$
T_f (K)	10.5	4.5
f	2.7	3.0
Assuming $\tau_0 = 10^{-7}$ s:		
E_a/k_B (K)	67.6(9)	17.1(9)
T_0 (K)	7.74(7)	4.01(8)
Assuming $\tau_0 = 10^{-11}$ s:		
E_a/k_B (K)	119.6(9)	68.2(8)
T_0 (K)	6.20(3)	2.21(4)
Assuming $\tau_0 = 10^{-13}$ s:		
E_a/k_B (K)	184.3(8)	105.7(5)
T_0 (K)	4.68(4)	1.33(2)
Θ_{CW} (K)	−27.28(14)	−13.23(3)
μ_{Eff} (μ_B)	10.69	10.79
M_0 (emu g^{-1})	0.8311(8)	2.111(3)
S (emu g^{-1})	0.0068(3)	0.0148(4)
RRR	1.1	—

magnetization of the Tb compound deviate below $T = 12$ K (figure 4(a)). The transition temperature (T_T) is obtained as a maximum of d(χT)/dT for $\mu_0 H = 100$ Oe, and is equal to $T_T = 10.5$ K. This value is close to the ordering temperature for Gd_2PdGe_3 ($T_T = 10$ K) [2]. The transition temperature for $Dy_2Pd_{1.25}Ge_{2.75}$ is estimated in the same way. The value of T_T shifts to lower temperatures with increasing $\mu_0 H$. Moreover, the value of T_T obtained from plot in figure 4(b) is more than twice as small as for $Tb_2Pd_{1.25}Ge_{2.75}$ ($T_T = 4.5$ K). The inset of figure 4(a) displays the field dependence of $M(H)$ at $T = 2$ K for $Tb_2Pd_{1.25}Ge_{2.75}$. It is obvious that the magnetization curve does not saturate, even at the highest applied field ($\mu_0 H = 9$ T). This phenomenon can be explained by the absence of long-range magnetic ordering, which agrees with spin–glass like character of $Tb_2Pd_{1.25}Ge_{2.75}$. A similar effect can be observed for $Dy_2Pd_{1.25}Ge_{2.75}$ (inset of figure 4(b)). Both compounds show a well-defined peak of $\chi(T)$ at low temperatures, which looks similar to the typical temperature dependence of the susceptibility for an antiferromagnetic material [10]. However, for a non-frustrated magnet the value of $|\theta_{cw}|$ is comparable to T_N. Both $Tb_2Pd_{1.25}Ge_{2.75}$ and $Dy_2Pd_{1.25}Ge_{2.75}$ have transition temperatures approximately three times smaller than $|\theta_{CW}|$. The empirical measure of frustration ($f = |\theta_{cw}|/T_T$) is much larger than 1 in both cases, suggesting magnetic frustration [11]. This feature, together with Pd–Ge site disorder and the possible presence of stacking faults, suggests that both compounds are spin–glass like materials and thus the observed magnetization drop below T_T results from a spin-freezing transition.

To confirm this hypothesis, measurements of the time-dependent remnant magnetization in the isothermal process for $Tb_2Pd_{1.25}Ge_{2.75}$ and $Dy_2Pd_{1.25}Ge_{2.75}$ were performed (figures 5(a) and (b) respectively). The time evolution of the magnetization resulting from slow relaxation is observed for both samples for T below freezing temperature. This behavior is known as the ageing effect and it is one of the crucial features in spin–glass-like materials [12–15]. Obtained curves

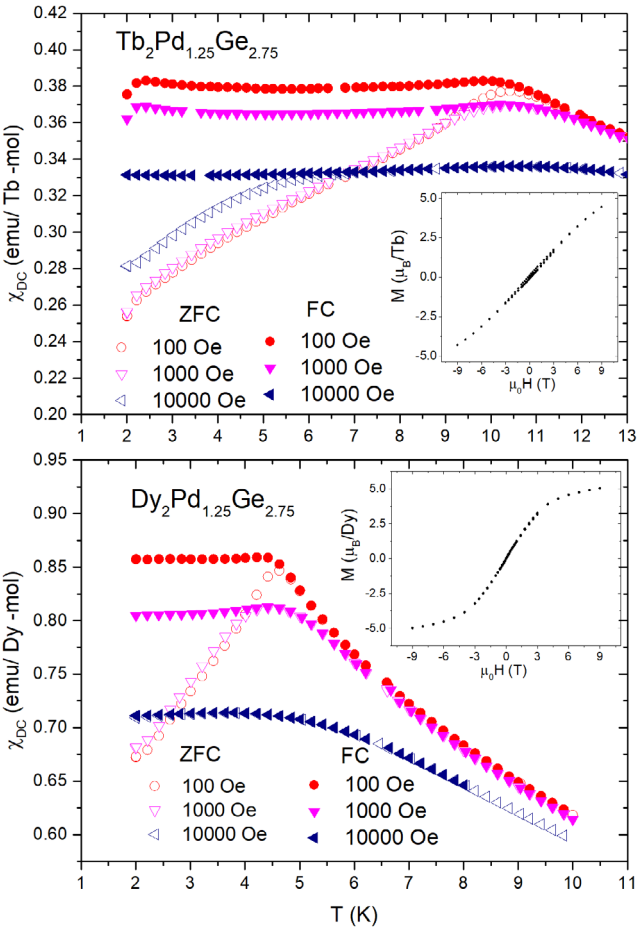

Figure 4. The difference between ZFC and FC magnetic susceptibility of $Tb_2Pd_{1.25}Ge_{2.75}$ and $Dy_2Pd_{1.25}Ge_{2.75}$ at various values of applied magnetic field. The transition temperature, defined here as the point of divergence between ZFC and FC curves decreases with increasing magnetic field. Insets shows $M(H)$ curves for $Tb_2Pd_{1.25}Ge_{2.75}$ and $Dy_2Pd_{1.25}Ge_{2.75}$ at 2 K. A small hysteresis is observed in both materials, with coercivity of $\mu_0 H_c \approx 0.2$ T for Tb- and $\mu_0 H_c \approx 0.02$ T for Dy-bearing sample.

may be fitted by the logarithmic function of time: $M(t) = M_0 + S\ln(t/t_0 + 1)$, where M_0 is magnetization at $t = 0$ and S is the magnetic viscosity. The reference time t_0 depends on the measuring conditions and has only limited physical relevance [12, 14]. The best fitting results obtained by using the least–squares method are shown by solid lines in figure 5. Estimated values of the zero-field magnetization and magnetic viscosity are collected in table 2. These values are comparable to the ones reported for other spin–glass-like compounds [12–15]. Another important feature of spin–glass-like behavior is shown in figure 6: the real part of the ac magnetic susceptibility exhibits a strong dependency of the magnetic transition on the frequency of the ac excitation field. The ac magnetic susceptibility was measured at frequencies $\upsilon = 19, 66, 233, 816, 2856$ and 10 000 Hz (logarithmic spacing) at an applied dc magnetic field $H_{dc} = 5$ Oe with $H_{ac} = 3$ Oe ac excitations, in a temperature range $T = 10$–16 K and $T = 4$–8 K for $Tb_2Pd_{1.25}Ge_{2.75}$ and $Dy_2Pd_{1.25}Ge_{2.75}$, respectively. In both cases the maximum in M' increases and shifts towards lower temperature as the frequency of the excitation field is decreased. The frequency

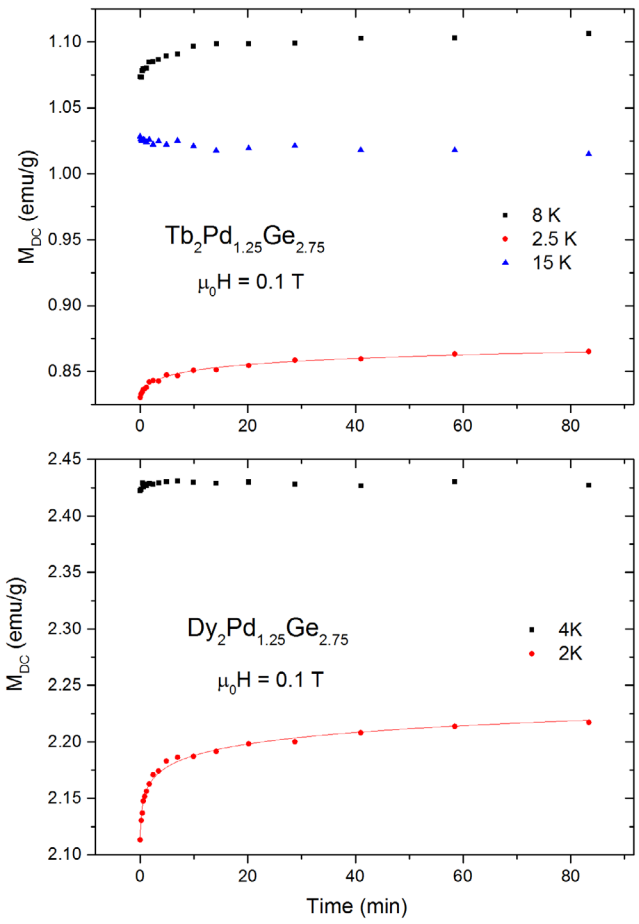

Figure 5. Time dependent remnant magnetization behavior for $Tb_2Pd_{1.25}Ge_{2.75}$ and $Dy_2Pd_{1.25}Ge_{2.75}$. Solid lines represent fits to equation $M(t) = M_0 + S\ln(t/t_0 + 1)$.

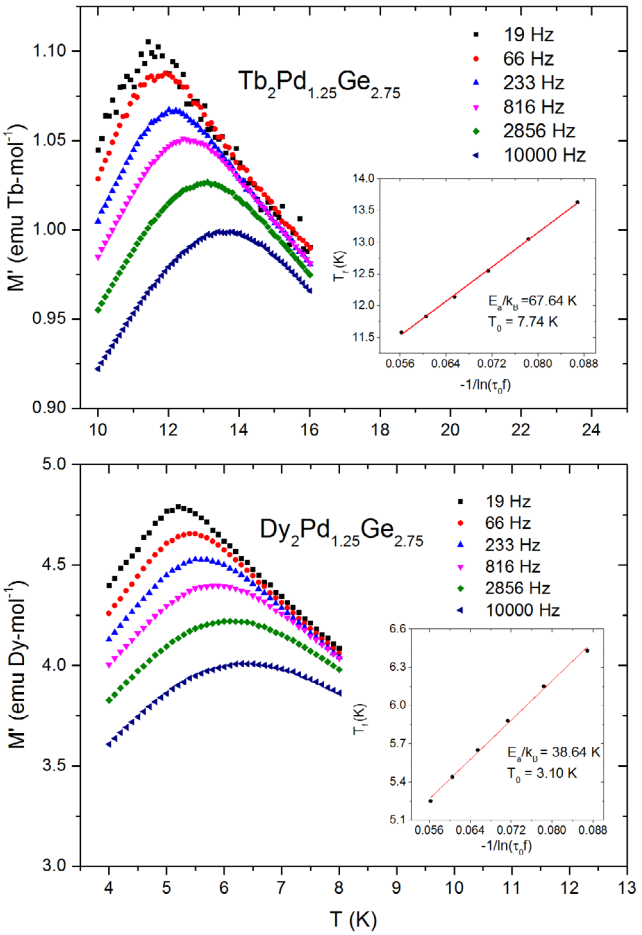

Figure 6. Temperature dependence of the real part of the ac magnetic susceptibility χ (T) for $Tb_2Pd_{1.25}Ge_{2.75}$ and $Dy_2Pd_{1.25}Ge_{2.75}$. Insets show plots of the freezing temperature (T_f) versus $1/\ln(\tau_0 f)$ with a Vogel–Fulcher law fit (red solid line).

(υ) dependence of the freezing temperature can be described by the empirical Vogel–Fulcher law:

$$T_f = T_0 - \frac{E_a}{k_B}\frac{1}{\ln(\tau_0\upsilon)},$$

with three fitting parameters: activation energy E_a (k_B is the Boltzman constant), Vogel—Fulcher temperature T_0 and intrinsic relaxation time τ_0 [15–17]. The last of these parameters can vary from $\tau_0 = 10^{-7}$ s for cluster glass compounds to $\tau_0 = 10^{-13}$ s for spin–glass materials. Plots of the freezing temperature versus $1/\ln(\tau_0\upsilon)$ for an assumed value of $\tau_0 = 10^{-11}$ s are shown in insets of figure 6. The calculated values of activation energy (presented in table 2) are similar to observed in RE_2PdSi_3 (RE = Tb, Dy), and have an order of magnitude that is typical for spin–glass materials [15, 17].

Heat capacity (C_p) measurements for $Tb_2Pd_{1.25}Ge_{2.75}$ and $Dy_2Pd_{1.25}Ge_{2.75}$ are shown in figure 7. In both cases at room temperature C_p reaches the expected Dulong–Petit law value, $3\,nR \approx 150$ J mol^{-1} K^{-1}, where n is the number of atoms per formula unit ($n = 6$) and R is the gas constant ($R = 8.314$ J mol^{-1} K^{-1}). The insets of figure 7 show the dependence of C_p/T at low temperatures. Both samples have a well-defined upturn at about the freezing temperature, which confirms that $RE_2Pd_{1.25}Ge_{2.75}$ (RE = Tb, Dy) can be classified as spin-glass like materials. In both cases the C_p peak is only weakly affected by the applied magnetic field.

The temperature dependence of the electrical resistivity (ρ) for $Tb_2Pd_{1.25}Ge_{2.75}$ is presented in figure 8. For temperatures above $T = 75$ K, $\rho(T)$ weakly decreases and exhibits the expected metallic behavior without any other noteworthy features. As the temperature decreases further, the electrical resistivity goes through cusps, which can be interpreted as a reduction of spin disorder scattering upon a magnetic transition. This feature is also observed in other compounds of the RE_2PdGe_3 family (RE = Ce, Nd, Gd) [2, 3, 18]. However, the value of transition temperature for $\rho(T)$ (the inset of figure 8) does not agree with that obtained from magnetization and heat capacity measurements, likely because there is no long-range spatial correlation function due to the lack of a periodically ordered state. This would suggest that disorder near the freezing temperature, still has a significant contribution to the electron scattering [19]. The calculated value of the residual resistivity ratio (RRR = $\rho_{(300K)}/\rho_{(2K)}$) is 1.1, which is typical for polycrystalline samples with internal defects or disorder. The magnetoresistance, which is defined as $MR = [\rho(H) - \rho(0)]/\rho(0)$ was measured as a

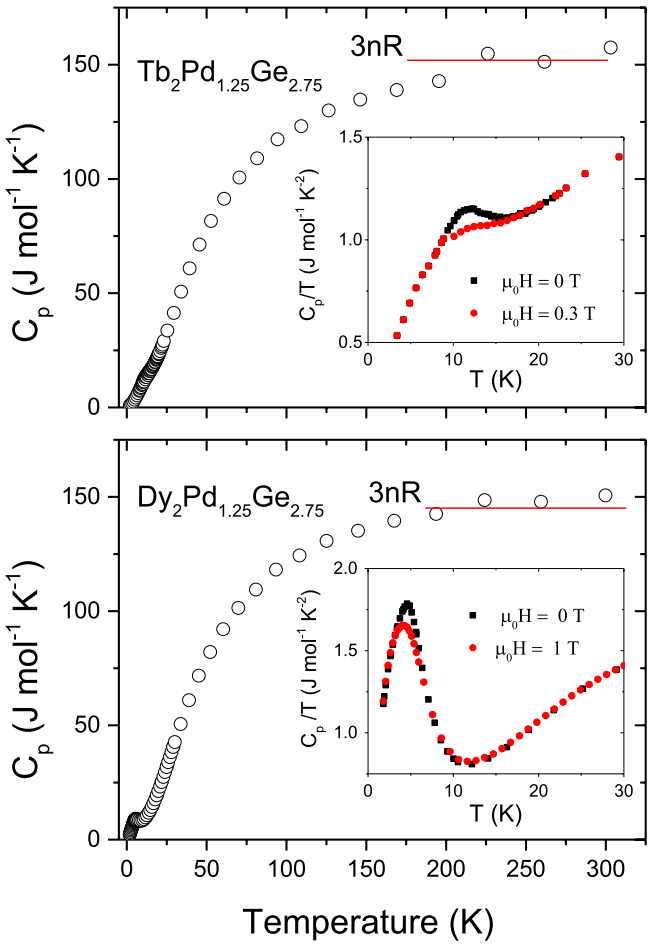

Figure 7. Temperature dependence of the heat capacity (C_p) for $Tb_2Pd_{1.25}Ge_{2.75}$ and $Dy_2Pd_{1.25}Ge_{2.75}$. Insets show plots of C_p/T versus T at low temperatures measured with and without applied magnetic field.

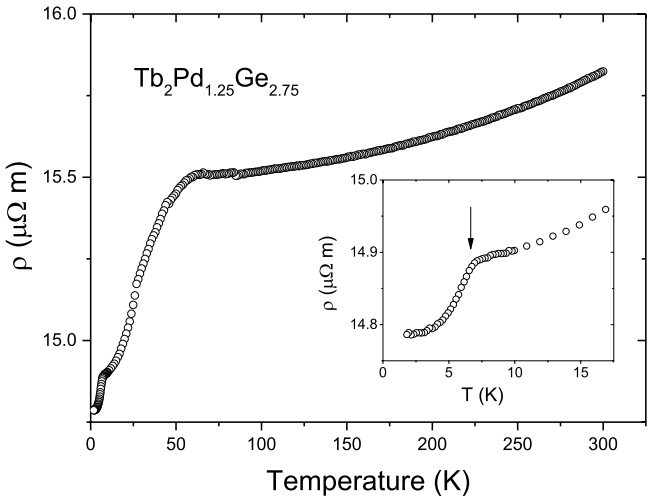

Figure 8. Electrical resistivity for $Tb_2Pd_{1.25}Ge_{2.75}$ measured at zero magnetic field. The inset shows the low temperature $\rho(T)$ dependence.

function of magnetic field at selected temperatures near the freezing temperature for $Tb_2Pd_{1.25}Ge_{2.75}$ sample (figure 9). The sign of the magnetoresistance is negative and is varying

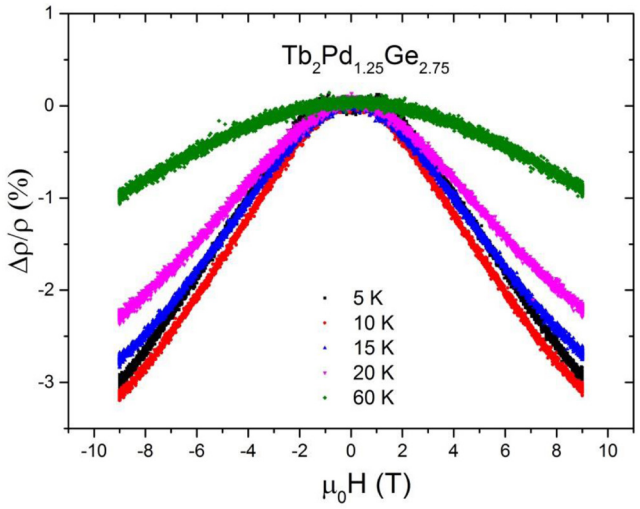

Figure 9. The magnetoresistance. $\Delta\rho/\rho = [\rho(H) - \rho(0)]/\rho(0)$, as a function of magnetic field for $Tb_2Pd_{1.25}Ge_{2.75}$.

approximately quadratically with the applied magnetic field for a wide range temperatures above the freezing temperature, which is expected for a state with a dominance of paramagnetic fluctuations [20]. Below T_f a qualitative change of the $MR(H)$ plot can be observed. This behavior was also reported for Nd_2PdGe_3 [3] and is likely caused by the decrease in spin-disorder scattering upon a magnetic transition, which is suppressed by an applied magnetic field.

Conclusions

We have synthetized polycrystalline samples of new intermetallic compounds $Tb_2Pd_{1.25}Ge_{2.75}$ and $Dy_2Pd_{1.25}Ge_{2.75}$ by an arc melting technique. Powder x-ray diffraction confirms that these compounds crystallize in a hexagonal structure (P6/*mmm*), a disordered variant of AlB_2 type, with refined lattice parameters $a = 4.228\,53(5)$ Å, $c = 3.942\,25(9)$ Å and $a = 4.225\,48(2)$ Å, $c = 3.903\,81(5)$ Å, for the Tb and Dy compounds respectively. The temperature dependence of the magnetic susceptibility obeys the Curie–Weiss law in the high temperature region for both compounds. The ac susceptibility and magnetic relaxation measurements give evidence for the formation of a spin–glass like state in $Tb_2Pd_{1.25}Ge_{2.75}$ and $Dy_2Pd_{1.25}Ge_{2.75}$ with freezing temperatures $T_f = 11.5$ K and $T_f = 4.5$ K respectively. These results are in good agreement with data obtained from heat capacity measurements. The temperature dependence of the electrical resistivity for the Tb compound shows metallic character. The low value of RRR = 1.1 is in agreement with the Pd–Ge site disorder.

Acknowledgments

This work was supported by Ministry of Science and Higher Education (Poland) under project 0142/DIA/2018/47 ('Diamentowy Grant'). MJ Winiarski was supported by the Foundation for Polish Science (FNP).

ORCID iDs

T Klimczuk https://orcid.org/0000-0002-7089-4631
M J Winiarski https://orcid.org/0000-0001-9083-8066

References

[1] Sampathkumaran E V, Majumdar S, Schneider W, Molodtsov S L and Laubschat C 2002 Superconductivity in Y_2PdGe_3 *Physica* B **312–3** 152–4
[2] Majumdar S, Kumar M M and Sampathkumaran E V 1999 Magnetic behavior of new compound Gd_2PdGe_3 *J. Alloys Compd.* **288** 61–4
[3] Majumdar S and Sampathkumaran E V 2001 Observation of enhanced magnetic transition temperature in Nd_2PdGe_3 and superconductivity in Y_2PdGe_3 *Phys. Rev.* B **63** 172407
[4] Seropegin Y D, Borisenko O L, Bodak O I, Nikiforov V F, Kovachikova M V and Kochetkov Y V 1994 Investigation of phase relationship and physical properties of Yb_Pd_Ge compounds *J. Alloys Compd.* **216** 259–63
[5] Momma K and Izumi F 2011 VESTA 3 for three-dimensional visualization of crystal, volumetric and morphology data *J. Appl. Crystallogr.* **44** 1272–6
[6] Klimczuk T, Weiwei Xie, Winiarski M J, Koziol R, Litzbarski L S, Luo H and Cava R J 2016 Crystal structure and physical properties of new Ca_2TGe_3 (T = Pd and Pt) germanides *J. Solid State Chem.* **243** 95–100
[7] Rodriguez-Carvajal J 1993 Recent advances in magnetic structure determination by neutron powder diffraction *Physica* B **192** 55–69
[8] Rodriguez-Carvajal J and Roisnel T 2004 Line broadening analysis using Fullprof∗: determination of microstructural properties *Mater. Sci. Forum* **443–4** 123–6
[9] Jensen J and Mackintosh A 1991 *Rare Earth Magnetism: Structures and Excitations* (Oxford: Clarendon)
[10] Spaldin N A 2011 *Magnetic Materials: Fundamentals and Applications* (Cambridge: Cambridge University Press)
[11] Ramirez A P 1994 Strongly geometrically frustrated magnets *Annu. Rev. Mater. Sci.* **24** 453–80
[12] Guang-Hui H, Ling-Wei L and Umehara I 2016 Pressure effect on magnetic phase transition and spin-glass-like behavior of $GdCo_2B_2$ *Chin. Phys.* B **25** 067501
[13] Sarkar S, Mondal A, Giri N and Ray R 2019 Spin glass like transition and the exchange bias effect in Co_3O_4 nans anchored onto graphene sheets *Phys. Chem. Chem. Phys.* **21** 260
[14] Harikrishnan S, Rößler S, Kumar C M N, Xiao Y, Bhat H L, Rößler U K, Steglich F, Wirth S and Elizabeth S 2010 Memory effect in $Dy_{0.5}Sr_{0.5}MnO_3$ single crystals *J. Phys.: Condens. Matter* **22** 3460002
[15] Li D X, Nimori S, Shiokawa Y, Haga Y, Yamamoto E and Onuki Y 2003 AC susceptibility and magnetic relaxation of R_2PdSi_3 *Phys. Rev.* B **68** 012413
[16] Górnicka K, Kolincio K K and Klimczuk T 2018 Spin-glass behavior in a binary Pr_3Ir intermetallic compound *Intermetallics* **100** 63–9
[17] Klimczuk T, Zandbergen H W, Huang Q, McQueen T M, Ronning F, Kusz B, Thompson J D and Cava R J 2009 Cluster—glass behavior of highly oxygen deficient perovskite $BaBi_{0.28}Co_{0.72}O_{2.2}$ *J. Phys.: Condens Matter* **21** 105801
[18] Baumbach R E, Gallagher A, Besara T, Sun J, Siegrist T, Singh D J, Thompson J D, Ronning F and Bauer E D 2015 Complex magnetism and strong electronic correlations in Ce_2PdGe_3 *Phys. Rev.* B **91** 035102
[19] Mydosh J A 1993 *Spin Glasses: an Experimental Introduction* (London: Taylor & Francis)
[20] Chattopadhyay M K, Arora P and Roy S B 2012 The magnetotransport properties of the intermetallic compound $GdCu_6$ *J. Phys.: Condens. Matter* **24** 146004